



HAL
open science

A Multilevel Schwarz Preconditioner Based on a Hierarchy of Robust Coarse Spaces

Hussam Al Daas, Laura Grigori, Pierre Jolivet, Pierre-Henri Tournier

► **To cite this version:**

Hussam Al Daas, Laura Grigori, Pierre Jolivet, Pierre-Henri Tournier. A Multilevel Schwarz Preconditioner Based on a Hierarchy of Robust Coarse Spaces. 2019. hal-02151184v1

HAL Id: hal-02151184

<https://hal.science/hal-02151184v1>

Preprint submitted on 7 Jun 2019 (v1), last revised 7 Dec 2020 (v2)

HAL is a multi-disciplinary open access archive for the deposit and dissemination of scientific research documents, whether they are published or not. The documents may come from teaching and research institutions in France or abroad, or from public or private research centers.

L'archive ouverte pluridisciplinaire **HAL**, est destinée au dépôt et à la diffusion de documents scientifiques de niveau recherche, publiés ou non, émanant des établissements d'enseignement et de recherche français ou étrangers, des laboratoires publics ou privés.

A MULTILEVEL SCHWARZ PRECONDITIONER BASED ON A HIERARCHY OF ROBUST COARSE SPACES*

HUSSAM AL DAAS[†], LAURA GRIGORI[‡], PIERRE JOLIVET[§], AND PIERRE-HENRI
TOURNIER[¶]

Abstract. In this paper we present a multilevel preconditioner based on overlapping Schwarz methods for symmetric positive definite (SPD) matrices. Robust two-level Schwarz preconditioners exist in the literature to guarantee fast convergence of Krylov methods. As long as the dimension of the coarse space is reasonable, that is, exact solvers can be used efficiently, two-level methods scale well on parallel architectures. However, the factorization of the coarse space matrix may become costly at scale. An alternative is then to use an iterative method on the second level, combined with an algebraic preconditioner, such as a one-level additive Schwarz preconditioner. Nevertheless, the condition number of the resulting preconditioned coarse space matrix may still be large. One of the difficulties of using more advanced methods, like algebraic multigrid or even two-level overlapping Schwarz methods, to solve the coarse problem is that the matrix does not arise from a partial differential equation (PDE) anymore. We introduce in this paper a robust multilevel additive Schwarz preconditioner where at each level the condition number is bounded, ensuring a fast convergence for each nested solver. Furthermore, our construction does not require any additional information than for building a two-level method, and may thus be seen as an algebraic extension.

Key words. domain decomposition, multilevel, elliptic problems, subspace correction

AMS subject classifications. 65F08, 65F10, 65N55

1. Introduction. We consider the solution of a linear system of equations

$$(1.1) \quad Ax = b,$$

where $A \in \mathbb{R}^{n \times n}$ is a symmetric positive definite (SPD) matrix, $b \in \mathbb{R}^n$ is the right-hand side, and $x \in \mathbb{R}^n$ is the vector of unknowns. To enhance convergence, it is common to solve the preconditioned system

$$M^{-1}Ax = M^{-1}b.$$

Standard domain decomposition preconditioners such as block Jacobi, additive Schwarz, and restricted additive Schwarz methods are widely used [31, 9, 8]. In a parallel framework, such preconditioners have the advantage of relatively low communication costs. However, their role in lowering the condition number of the system typically deteriorates when the number of subdomains increases. Multilevel approaches have shown a large impact on enhancing the convergence of Krylov methods [32, 12, 7, 25, 20, 10, 21, 1, 15, 23]. In multigrid and domain decomposition communities, multilevel methods have proven their capacity of scaling up to large numbers of processors and tackling ill-conditioned systems [35, 4, 19]. While some preconditioners are purely algebraic [7, 20, 10, 26, 29, 16, 1], several multilevel methods are based on hierarchical meshing in both multigrid and domain decomposition communities [33, 9, 25, 15, 23]. Mesh coarsening depends on the geometry of the problem. One

*Submitted to the editors June 5, 2019.

[†]ALPINES, INRIA, Paris, France (aldaas.hussam@gmail.com, <https://www.aldaas.net>).

[‡]ALPINES, INRIA, Paris, France (laura.grigori@inria.fr, <https://who.rocq.inria.fr/Laura.Grigori>).

[§]IRIT, CNRS, Toulouse, France (pierre.jolivet@enseeiht.fr, <http://jolivet.perso.enseeiht.fr>).

[¶]LJLL, CNRS, Paris, France (tournier@ljl.math.upmc.fr).

39 has to be careful when choosing a hierarchical structure since it can have a signifi-
 40 cant impact on the iteration count [23, 25]. In [23], the authors propose a multilevel
 41 Schwarz domain decomposition solver for the elasticity problem. Based on a heuristic
 42 approach and following the maximum independent set method [2], they coarsen the
 43 fine mesh while preserving the boundary in order to obtain a two-level method. This
 44 strategy is repeated recursively to build several levels. However, they do not provide a
 45 bound on the condition number of the preconditioned matrix of the multilevel method.
 46 Multilevel domain decomposition methods are mostly based on non-overlapping ap-
 47 proaches [33, 9, 25, 23, 35, 4]. Two-level overlapping domain decomposition methods
 48 are well studied and provide robust convergence estimates [32, 12, 5]. However, ex-
 49 tending such a construction to more than two levels while preserving robustness is not
 50 straightforward. In [6], the authors propose an algebraic multilevel additive Schwarz
 51 method. Their approach is inspired by algebraic multigrid strategies. One drawback
 52 of it is that it is sensitive to the number of subdomains. In [15], the authors suggest
 53 applying the two-level Generalized Dryja–Smith–Widlund preconditioner recursively
 54 to build a multilevel method. In this case, the condition number bound of the two-
 55 level approach depends on the width of the overlap, the diameter of discretization
 56 elements, and the diameter of the subdomains. They focus on the preconditioner for
 57 the three-level case. One drawback of their approach is that the three-level precon-
 58 ditioner requires more iterations than the two-level variant. In this paper, the only
 59 information from the PDE needed for the construction of the preconditioner consists
 60 of the local Neumann matrices at the fine level. These matrices correspond to the
 61 integration of the bilinear form in the weak formulation of the studied PDE on the
 62 subdomain-decomposed input mesh. No further information is necessary: except on
 63 the fine level, our method is algebraic and does not depend on any coarsened mesh or
 64 auxiliary discretized operator.

65 Our preconditioner is based on a hierarchy of coarse spaces and is defined as fol-
 66 lowing. At the first level, the set of unknowns is partitioned into N_1 subdomains and
 67 each subdomain has an associated matrix $A_{1,j} = R_{1,j} A R_{1,j}^\top$ obtained by using appro-
 68 priate restriction and prolongation operators $R_{1,j}$ and $R_{1,j}^\top$ respectively, defined in the
 69 following section. The preconditioner is formed as an additive Schwarz preconditioner
 70 coupled with an additive coarse space correction, defined as,

$$71 \quad M^{-1} = M_1^{-1} = V_1 A_2^{-1} V_1^\top + \sum_{j=1}^{N_1} R_{1,j}^\top A_{1,j}^{-1} R_{1,j},$$

72 where V_1 is a tall-and-skinny matrix spanning a coarse space obtained by solving for
 73 each subdomain $j = 1$ to N_1 a generalized eigenvalue problem involving the matrix
 74 $A_{1,j}$ and the Neumann matrix associated with subdomain j . The coarse space matrix
 75 is $A_2 = V_1^\top A V_1$. This is equivalent to the GenEO preconditioner, and is described
 76 in detail in [32] and recalled briefly in section 2. The dimension of the coarse space
 77 is proportional to the number of subdomains N_1 . When it increases, factorizing A_2
 78 by using a direct method becomes prohibitive, and hence the application of A_2^{-1} to a
 79 vector should also be performed through an iterative method.

80 Our multilevel approach defines a hierarchy of coarse spaces V_i and coarse space
 81 matrices A_i for $i = 2$ to any depth $L + 1$, and defines a preconditioner M_i^{-1} such that
 82 the condition number of $M_i^{-1} A_i$ is bounded. The depth $L + 1$ is chosen such that the
 83 coarse space matrix A_{L+1} can be factorized efficiently by using a direct method. At
 84 each level i , the graph of the coarse space matrix A_i is partitioned into N_i subdomains,
 85 and each subdomain j is associated with a local matrix $A_{i,j} = R_{i,j} A_i R_{i,j}^\top$ obtained by

86 using appropriate restriction and prolongation operators $R_{i,j}$ and $R_{i,j}^\top$, respectively.
 87 The preconditioner at level i is defined as,

$$88 \quad M_i^{-1} = V_i A_{i+1}^{-1} V_i^\top + \sum_{j=1}^{N_i} R_{i,j}^\top A_{i,j}^{-1} R_{i,j},$$

89 where the coarse space matrix is $A_{i+1} = V_i^\top A_i V_i$.

90 One of the main contributions of the paper concerns the construction of the
 91 hierarchy of coarse spaces V_i for levels i going from 2 to L , that are built algebraically
 92 from the coarse space of the previous level V_{i-1} . This construction is based on the
 93 definition of local symmetric positive semi-definite (SPSD) matrices associated with
 94 each subdomain j at each level i that we introduce in this paper. These matrices are
 95 obtained by using the local SPSP matrices of the previous level $i-1$ and the previous
 96 coarse space V_{i-1} . They are then involved, with the local matrices $A_{i,j}$, in concurrent
 97 generalized eigenvalue problems solved for each subdomain j that allows to compute
 98 the local eigenvectors contributing to the coarse space V_i .

99 We show in [Theorem 5.3, section 5](#), that the condition number of $M_i^{-1} A_i$ is
 100 bounded and depends on the maximum number of subdomains at the first level that
 101 share an unknown, the number of distinct colors required to color the graph of A_i so
 102 that $\{span\{R_{i,j}^\top\}\}_{1 \leq j \leq N_i}$ of the same color are mutually A_i -orthogonal, and a user
 103 defined tolerance τ . It is thus independent of the number of subdomains N_i .

104 The main contribution of this paper is based on the combination of two previous
 105 works on two-level additive Schwarz methods [\[3, 32\]](#). The coarse space proposed in
 106 [\[32\]](#) guarantees an upper bound on the condition number that can be prescribed by
 107 the user. The SPSP splitting in the context of domain decomposition presented in
 108 [\[3\]](#) provides an algebraic view for the construction of coarse spaces. The combination
 109 of these two works leads to a robust multilevel additive Schwarz method. Here,
 110 robustness refers to the fact that at each level, an upper bound on the condition
 111 number of the associated matrix can be prescribed by the user a priori. The rest
 112 of the paper is organized as follows. In the next section, we present the notations
 113 used throughout the paper. In [section 2](#), we present a brief review of the theory of
 114 one- and two-level additive Schwarz methods. We extend in [section 3](#) the class of
 115 SPSP splitting matrices presented in [\[3\]](#) in order to make it suitable for multilevel
 116 methods. Afterwards, we define the coarse space at level i based on the extended
 117 class of local SPSP splitting matrices associated with this level. [Section 4](#) describes
 118 the partitioning of the domain at level $i+1$ from the partitioning at level i . In
 119 [Section 5](#), we explain the computation of the local SPSP matrices associated with each
 120 subdomain at level $i+1$. We compute them using those associated with subdomains
 121 at level i . [Section 6](#) presents numerical experiments on highly challenging diffusion
 122 and linear elasticity problems in two- and three-dimensional problems. We illustrate
 123 the theoretical robustness and practical usage of our proposed method by performing
 124 strong scalability tests up to 8,192 processes.

125 **Context and notation.** By convention, the finest level, on which [\(1.1\)](#) is
 126 defined, is the first level. A subscript index is used in order to specify which level
 127 an entity is defined on. In the case where additional subscripts are used, the first
 128 subscript always denotes the level. For the sake of clarity, we omit the subscript cor-
 129 responding to level 1 when it is clear from context, e.g., matrix A . Furthermore, the
 130 subscripts i and j always refer to a specific level i and its subdomain j , respectively.
 131 The number of levels is $L+1$. Let $A_i \in \mathbb{R}^{n_i \times n_i}$ denote symmetric positive definite

132 matrices, each corresponding to level $i = 1, \dots, L+1$. We suppose that a direct solver
 133 can be used at level $L+1$ to compute an exact factorization of A_{L+1} .

134 Let $B \in \mathbb{R}^{p \times q}$ be a matrix. Let $P \subset \llbracket 1; p \rrbracket$ and $Q \subset \llbracket 1; q \rrbracket$ be two sets of
 135 indices. The concatenation of P and Q is represented by $[P, Q]$. We note that the
 136 order of the concatenation is important. $B(P, :)$ is the submatrix of B formed by
 137 the rows whose indices belong to P . $B(:, Q)$ is the submatrix of B formed by the
 138 columns whose indices belong to Q . $B(P, Q) = (B(P, :))(:, Q)$. The identity matrix
 139 of size p is denoted I_p . We suppose that the graph of A_i is partitioned into N_i non-
 140 overlapping subdomains, where $N_i \ll n_i$ and $N_{i+1} \leq N_i$ for $i = 1, \dots, L$. We note that
 141 partitioning at level 1 can be performed by using a graph partitioning library such as
 142 ParMETIS [22] or PT-SCOTCH [11]. Partitioning at greater levels will be described
 143 later in section 4. In the following, we define for each level $i = 1, \dots, L$ notations
 144 for subsets and restriction operators that are associated with the partitioning. Let
 145 $\Omega_i = \llbracket 1; n_i \rrbracket$ be the set of unknowns at level i and let $\Omega_{i,j,I}$ for $j = 1, \dots, N_i$ be the
 146 subset of Ω_i that represents the unknowns in subdomain j . We refer to $\Omega_{i,j,I}$ as the
 147 *interior unknowns* of subdomain j . Let $\Gamma_{i,j}$ for $j = 1, \dots, N_i$ be the subset of Ω_i that
 148 represents the neighbor unknowns of subdomain j , i.e., the unknowns at distance 1
 149 from subdomain j through the graph of A_i . We refer to $\Gamma_{i,j}$ as the *overlapping*
 150 *unknowns* of subdomain j . We denote $\Omega_{i,j} = [\Omega_{i,j,I}, \Gamma_{i,j}]$, for $j = 1, \dots, N_i$, the
 151 concatenation of interior and overlapping unknowns of subdomain j . We denote
 152 $\Delta_{i,j}$, for $j = 1, \dots, N_i$, the complementary of $\Omega_{i,j}$ in Ω_i , i.e., $\Delta_{i,j} = \Omega_i \setminus \Omega_{i,j}$. In
 153 Figure 1.1, a triangular mesh is used to discretize a square domain. The set of
 154 nodes of the mesh is partitioned into 16 disjoint subsets $\Omega_{1,j,I}$, which represent a
 155 non-overlapping decomposition, for $j = 1, \dots, 16$ (left). On the left, a matrix A_1
 156 whose connectivity graph corresponds to the mesh is illustrated. The submatrix
 157 $A_1(\Omega_{1,j,I}, \Omega_{1,j,I})$ is associated with the non-overlapping subdomain j . Each submatrix
 158 $A_1(\Omega_{1,j,I}, \Omega_{1,j,I})$ is colored with a distinct color. The same color is used to color the
 159 region that contains the nodes in the non-overlapping subdomain $\Omega_{1,j,I}$. Note that
 160 if two subdomains j_1, j_2 are neighbors, the submatrix $A_1(\Omega_{1,j_1,I}, \Omega_{1,j_2,I})$ has nonzero
 161 elements. For $j = 1, \dots, N_i$, we denote by $n_{i,j,I}$, $\gamma_{i,j}$ and $n_{i,j}$ the cardinality of $\Omega_{i,j,I}$,
 162 $\Gamma_{i,j}$ and $\Omega_{i,j}$ respectively.
 163 Let $R_{i,j,I} \in \mathbb{R}^{n_{i,j,I} \times n_i}$ be defined as $R_{i,j,I} = I_{n_i}(\Omega_{i,j,I}, :)$.
 164 Let $R_{i,j,\Gamma} \in \mathbb{R}^{\gamma_{i,j} \times n_i}$ be defined as $R_{i,j,\Gamma} = I_{n_i}(\Gamma_{i,j}, :)$.
 165 Let $R_{i,j} \in \mathbb{R}^{n_{i,j} \times n_i}$ be defined as $R_{i,j} = I_{n_i}(\Omega_{i,j}, :)$.
 166 Let $R_{i,j,\Delta} \in \mathbb{R}^{(n_i - n_{i,j}) \times n_i}$ be defined as $R_{i,j,\Delta} = I_{n_i}(\Delta_{i,j}, :)$.
 167 Let $\mathcal{P}_{i,j} = I_{n_i}([\Omega_{i,j,I}, \Gamma_{i,j}, \Delta_{i,j}], :) \in \mathbb{R}^{n_i \times n_i}$, be a permutation matrix associated
 168 with the subdomain j , for $j = 1, \dots, N_i$. The matrix of the overlapping subdomain j ,
 169 $R_{i,j} A_i R_{i,j}^\top$, is denoted $A_{i,j}$. We denote $D_{i,j} \in \mathbb{R}^{n_{i,j} \times n_{i,j}}$, $j = 1, \dots, N_i$, any set of
 170 non-negative diagonal matrices such that

$$171 \quad I_{n_i} = \sum_{j=1}^{N_i} R_{i,j}^\top D_{i,j} R_{i,j}.$$

172 We refer to $\{D_{i,j}\}_{1 \leq j \leq N_i}$ as the algebraic partition of unity. Let $V_i \in \mathbb{R}^{n_i \times n_{i+1}}$ be
 173 a tall-and-skinny matrix of full rank. We denote \mathcal{S}_i the subspace spanned by the
 174 columns of V_i . This subspace will stand for the coarse space associated with level i .
 175 By convention, we refer to \mathcal{S}_i as subdomain 0 at level i . Thus, we have $n_{i,0} = n_{i+1}$.

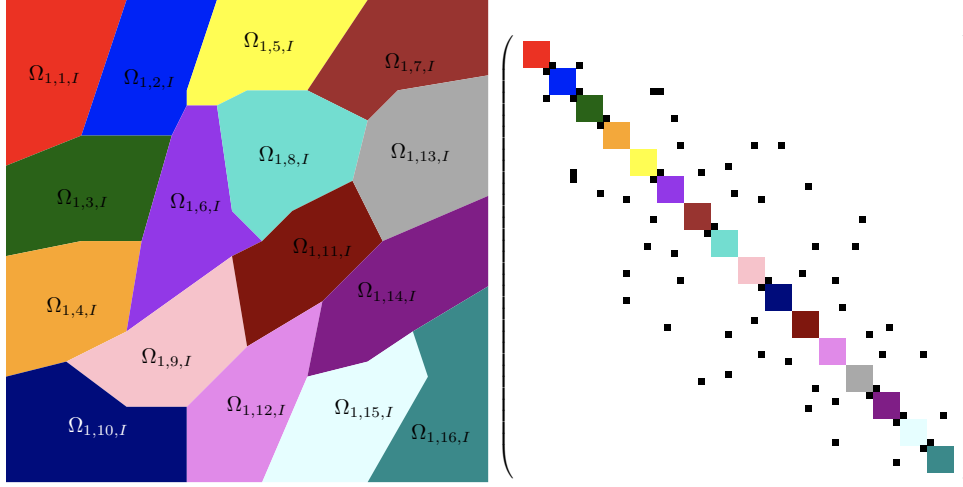


FIG. 1.1. *Left: a triangular mesh is used to discretize the unit square. The set of nodes of the mesh is partitioned into 16 disjoint subsets, non-overlapping subdomains, $\Omega_{1,j,I}$ for $j = 1, \dots, 16$. Right: Illustration of the matrix A_1 whose connectivity graph corresponds to the mesh on the left. The diagonal block j of A_1 corresponds to the non-overlapping subdomain $\Omega_{1,j,I}$. Each submatrix $A_1(\Omega_{1,j,I}, \Omega_{1,j,I})$ is colored with a distinct color. The same color is used to color the region of the square that contains nodes in $\Omega_{1,j,I}$.*

176 The interpolation operator at level i is defined as:

$$\begin{aligned}
 & \mathcal{R}_{i,2}: \prod_{j=0}^{N_i} \mathbb{R}^{n_{i,j}} \rightarrow \mathbb{R}^{n_i} \\
 & (u_j)_{0 \leq j \leq N_i} \mapsto \sum_{j=0}^{N_i} R_{i,j}^\top u_j.
 \end{aligned}
 \tag{1.2}$$

179 Finally, we denote $\mathcal{V}_{i,j}$ the set of neighboring subdomains of each subdomain j at
 180 level i for $(i, j) \in \llbracket 1; L \rrbracket \times \llbracket 1; N_i \rrbracket$.

$$\mathcal{V}_{i,j} = \{k \in \llbracket 1; N_i \rrbracket : \Omega_{i,j} \cap \Omega_{i,k} \neq \emptyset\}.$$

182 As previously mentioned, partitioning at level 1 can be performed by graph parti-
 183 tioning libraries such as ParMETIS [22] or PT-SCOTCH [11]. Partitioning at further
 184 levels will be defined later: the sets $\Omega_{i,j,I}$, $\Omega_{i,j,\Gamma}$, $\Omega_{i,j}$, and $\Delta_{i,j}$ for $i > 1$ are defined
 185 in subsection 4.2. The coarse spaces \mathcal{S}_i as well as the projection and prolongation
 186 operators V_i^\top and V_i are defined in subsection 3.2. We suppose that the connectivity
 187 graph between the subdomains on each level is sparse. This assumption is not true in
 188 general, however, it is valid in structures based on locally constructed coarse spaces
 189 in domain decomposition as we show in this paper, see [18, Section 4.1 p.81] for the
 190 case of two levels.

191 **2. Background.** In this section, we review briefly several theoretical results
 192 related to additive Schwarz preconditioners. We introduce them for the sake of com-
 193 pleteness.

194 LEMMA 2.1 (fictitious subspace lemma). *Let $A \in \mathbb{R}^{n_A \times n_A}$, $B \in \mathbb{R}^{n_B \times n_B}$ be two*

195 symmetric positive definite matrices. Let \mathcal{R} be an operator defined as

$$\begin{aligned} 196 \quad & \mathcal{R}: \mathbb{R}^{n_B} \rightarrow \mathbb{R}^{n_A} \\ 197 \quad & v \mapsto \mathcal{R}v, \end{aligned}$$

198 and let \mathcal{R}^\top be its transpose. Suppose that the following conditions hold:

- 199 1. The operator \mathcal{R} is surjective.
- 200 2. There exists $c_u > 0$ such that

$$201 \quad (\mathcal{R}v)^\top A (\mathcal{R}v) \leq c_u v^\top B v, \quad \forall v \in \mathbb{R}^{n_B}.$$

- 202 3. There exists $c_l > 0$ such that for all $v_{n_A} \in \mathbb{R}^{n_A}, \exists v_{n_B} \in \mathbb{R}^{n_B} | v_{n_A} = \mathcal{R}v_{n_B}$
- 203 and

$$204 \quad c_l v_{n_B}^\top B v_{n_B} \leq (\mathcal{R}v_{n_B})^\top A (\mathcal{R}v_{n_B}) = v_{n_A}^\top A v_{n_A}.$$

205 Then, the spectrum of the operator $\mathcal{R}B^{-1}\mathcal{R}^\top A$ is contained in the segment $[c_l, c_u]$.

206 *Proof.* We refer the reader to [12, Lemma 7.4 p.164] or [28, 27, 13] for a detailed
207 proof. \square

208 LEMMA 2.2. The operator $\mathcal{R}_{i,2}$ as defined in (1.2) is surjective.

209 *Proof.* The proof follows from the definition of $\mathcal{R}_{i,2}$ (1.2). \square

210 LEMMA 2.3. Let $k_{i,c}$ for $i = 1, \dots, L$ be the minimum number of distinct colors
211 so that $\{\text{span}\{R_{i,j}^\top\}\}_{1 \leq j \leq N_i}$ of the same color are mutually A_i -orthogonal. Then, we
212 have

$$\begin{aligned} 214 \quad & (\mathcal{R}_{i,2}u_{\mathcal{B}_i})^\top A_i (\mathcal{R}_{i,2}u_{\mathcal{B}_i}) \\ 215 \quad & \leq (k_{i,c} + 1) \sum_{j=0}^{N_i} u_j^\top (R_{i,j} A_i R_{i,j}^\top) u_j, \quad \forall u_{\mathcal{B}_i} = (u_j)_{0 \leq j \leq N_i} \in \prod_{j=0}^{N_i} \mathbb{R}^{n_{i,j}}. \end{aligned}$$

217 *Proof.* We refer the reader to [9, Theorem 12 p.93] for a detailed proof. \square

218 We note that at level i , the number $k_{i,c}$ is smaller than the maximum number of
219 neighbors over the set of subdomains $\llbracket 1; N_i \rrbracket$

$$220 \quad k_{i,c} \leq \max_{1 \leq j \leq N_i} \#\mathcal{V}_{i,j}.$$

221 Due to the sparse structure of the connectivity graph between the subdomains at
222 level i , the maximum number of neighbors over the set of subdomains $\llbracket 1; N_i \rrbracket$ is
223 independent of the number of subdomains N_i . Then, so is $k_{i,c}$.

224 LEMMA 2.4. Let $u_{A_i} \in \mathbb{R}^{n_{A_i}}$ and $u_{\mathcal{B}_i} = \{u_j\}_{0 \leq j \leq N_i} \in \prod_{j=0}^{N_i} \mathbb{R}^{n_{i,j}}$ such that $u_{A_i} =$
225 $\mathcal{R}_{i,2}u_{\mathcal{B}_i}$. The additive Schwarz operator without any other restriction on the coarse
226 space \mathcal{S}_i verifies the following inequality

$$227 \quad \sum_{j=0}^{N_i} u_j^\top (R_{i,j} A_i R_{i,j}^\top) u_j \leq 2u_{A_i}^\top A_i u_{A_i} + (2k_{i,c} + 1) \sum_{j=1}^{N_i} u_j^\top R_{i,j} A_i R_{i,j}^\top u_j,$$

228 where $k_{i,c}$ is defined in Lemma 2.3.

229 *Proof.* We refer the reader to [12, Lemma 7.12, p. 175] to view the proof in
 230 detail. \square

231 **LEMMA 2.5.** *Let $A, B \in \mathbb{R}^{m \times m}$ be two symmetric positive semi-definite matrices.*
 232 *Let $\ker(A)$, $\text{range}(A)$ denote the null space and the range of A respectively.*
 233 *Let $\ker(B)$ denote the kernel of B . Let $L = \ker(A) \cap \ker(B)$, we denote $L^{\perp_{\ker(A)}}$*
 234 *the orthogonal complementary of L in $\ker(A)$. Let P_0 be an orthogonal projection*
 235 *on $\text{range}(A)$. Let τ be a positive real number. Consider the generalized eigenvalue*
 236 *problem,*

$$237 \quad P_0 B P_0 u_k = \lambda_k A u_k,$$

$$238 \quad (u_k, \lambda_k) \in \text{range}(A) \times \mathbb{R}.$$

239 Let P_τ be an orthogonal projection on the subspace

$$240 \quad Z = L^{\perp_{\ker(A)}} \oplus \text{span}\{u_k | \lambda_k > \tau\},$$

241 then, the following inequality holds:

$$242 \quad (2.1) \quad (u - P_\tau u)^\top B (u - P_\tau u) \leq \tau u^\top A u, \quad \forall u \in \mathbb{R}^m.$$

243 Furthermore, Z is the subspace of smallest dimension such that (2.1) holds.

244 *Proof.* We refer the reader to [3, Lemma 2.4] for a detailed proof. \square

245 **2.1. GenEO coarse space.** In [32, 12] the authors present the GenEO coarse
 246 space which relies on defining appropriate symmetric positive semi-definite (SPSD)
 247 matrices $\tilde{A}_j \in \mathbb{R}^{n \times n}$ for $j = 1, \dots, N$. These are the unassembled Neumann matrices,
 248 corresponding to the integration on each subdomain of the operator defined in the
 249 variational form of the PDE. These matrices are local, i.e., $R_{j,\Delta} \tilde{A}_j = 0$. Furthermore,
 250 they verify the relations

$$251 \quad u^\top \tilde{A}_j u \leq u^\top A u, \quad \forall u \in \mathbb{R}^n,$$

$$252 \quad u^\top \sum_{j=1}^N \tilde{A}_j u \leq k_{\text{GenEO}} u^\top A u, \quad \forall u \in \mathbb{R}^n,$$

253 where $k_{\text{GenEO}} \leq N$ is the maximum number of subdomains that share an unknown.

254 **2.2. Local SPSP splitting of an SPD matrix.** In [3], the authors present
 255 the local SPSP splitting of an SPD matrix. Given the permutation matrix \mathcal{P}_j , a local
 256 SPSP splitting matrix \tilde{A}_j of A associated with subdomain j is defined as

$$257 \quad (2.2) \quad \mathcal{P}_j \tilde{A}_j \mathcal{P}_j^\top = \begin{pmatrix} R_{j,I} A R_{j,I}^\top & R_{j,I} A R_{j,\Gamma}^\top \\ R_{j,\Gamma} A R_{j,I}^\top & \tilde{A}_\Gamma^j \\ & & 0 \end{pmatrix},$$

258 where $\tilde{A}_\Gamma^j \in \mathbb{R}^{\gamma_j \times \gamma_j}$ satisfies the two following conditions: For all $u \in \mathbb{R}^{\gamma_j}$,

- 259 • $u^\top (R_{j,\Gamma} A R_{j,I}^\top) (R_{j,I} A R_{j,I}^\top)^{-1} (R_{j,I} A R_{j,\Gamma}^\top) u \leq u^\top \tilde{A}_\Gamma^j u$
- 260 • $u^\top \tilde{A}_\Gamma^j u \leq u^\top \left((R_{j,\Gamma} A R_{j,\Gamma}^\top) - (R_{j,\Gamma} A R_{j,\Delta}^\top) (R_{j,\Delta} A R_{j,\Delta}^\top)^{-1} (R_{j,\Delta} A R_{j,\Gamma}^\top) \right) u.$

261 The authors prove that the matrices \tilde{A}_j defined in such a way verify the following
 262 relations:

$$263 \quad (2.3) \quad R_{j,\Delta}\tilde{A}_j = 0,$$

$$264 \quad (2.4) \quad u^\top \tilde{A}_j u \leq u^\top A u, \quad \forall u \in \mathbb{R}^n,$$

$$265 \quad (2.5) \quad u^\top \sum_{j=1}^N \tilde{A}_j u \leq k u^\top A u, \quad \forall u \in \mathbb{R}^n,$$

266
 267 where k is a number that depends on the local SPSD splitting matrices and can be
 268 at most equal to the number of subdomains $k \leq N$. The authors also show that the
 269 local matrices defined in GenEO [32, 12] can be seen as a local SPSD splitting.

270 In [3], the authors highlight that the key idea to construct a coarse space relies
 271 on the ability to identify the so-called local SPSD splitting matrices. They present
 272 a class of algebraically constructed coarse spaces based on the local SPSD splitting
 273 matrices. Moreover, this class can be extended to a larger variety of local SPSD
 274 matrices. This extension has the advantage of allowing to construct efficient coarse
 275 spaces for a multilevel structure in a practical way. This is discussed in the following
 276 section.

277 **3. Extension of the class of coarse spaces.** In this section we extend the
 278 class of coarse spaces presented in [3]. To do so, we present a class of matrices, that is
 279 larger than the class of local SPSD splitting matrices. This will be our main building
 280 block in the construction of efficient coarse spaces. Furthermore, this extension can
 281 lead to a straightforward construction of hierarchical coarse spaces in a multilevel
 282 Schwarz preconditioner setting.

283 **3.1. Extension of the class of local SPSD splitting matrices.** Regarding
 284 the two-level additive Schwarz method, the authors of [3] introduced the local SPSD
 285 splitting related to a subdomain as defined in (2.2). As it can be seen from the theory
 286 presented in that paper, it is not necessary to have the exact matrices $R_{j,I}AR_{j,I}^\top$,
 287 $R_{j,I}AR_{j,\Gamma}^\top$, and $R_{j,\Gamma}AR_{j,I}^\top$ in the definition of the local SPSD splitting in order to
 288 build an efficient coarse space. Indeed, the one and only necessary condition is to
 289 define for each subdomain j an SPSD matrix \tilde{A}_j for $j = 1, \dots, N$ such that:

$$290 \quad (3.1) \quad \begin{aligned} & R_{j,\Delta}\tilde{A}_j = 0, \\ & u^\top \sum_{j=1}^N \tilde{A}_j u \leq k u^\top A u, \forall u \in \mathbb{R}^n, \end{aligned}$$

291
 292 where k is a number that depends on the local SPSD matrices \tilde{A}_j for $j = 1, \dots, N$.
 293 The first condition means that \tilde{A}_j has the local SPSD structure associated with sub-
 294 domain j , i.e., it has the following form:

$$295 \quad \mathcal{P}_j \tilde{A}_j \mathcal{P}_j^\top = \begin{pmatrix} \tilde{A}_{I,\Gamma}^j & 0 \\ 0 & 0 \end{pmatrix},$$

296 where $\tilde{A}_{I,\Gamma}^j \in \mathbb{R}^{n_j \times n_j}$. The second condition is associated with the stable decom-
 297 position property [34, 12]. Note that with regard to the local SPSD matrices, the
 298 authors in [32] only use these two conditions. That is to say, with matrices that verify
 299 conditions (3.1) the construction of the coarse space is straightforward through the

theory presented in either [32] or [3]. To this end, we define in the following the local
 SPSPD (LSPSPD) matrix associated with subdomain j as well as the associated local
 filtering subspace that contributes to the coarse space.

DEFINITION 3.1 (local SPSPD matrices). *An SPSPD matrix $\tilde{A}_{i,j} \in \mathbb{R}^{n_i \times n_i}$ is called
 local SPSPD (LSPSPD) with respect to subdomain j if*

- $R_{i,j,\Delta} \tilde{A}_{i,j} = 0$,
 - $u^\top \sum_{j=1}^{N_i} \tilde{A}_{i,j} u \leq k_i u^\top A_i u$,
- where $k_i > 0$.

We note that the local SPSPD splitting matrices form a subset of the local SPSPD
 matrices.

3.2. Multilevel coarse spaces. This section summarizes the steps to be per-
 formed in order to construct the coarse space at level i once we have the LSPSPD
 matrices associated with each subdomain at that level.

DEFINITION 3.2 (coarse space based on LSPSPD matrices). *Let $\tilde{A}_{i,j} \in \mathbb{R}^{n_i \times n_i}$ for
 $j = 1, \dots, N_i$ be LSPSPD matrices. Let $D_{i,j} \in \mathbb{R}^{n_i \times j}$ for $j = 1, \dots, N_i$ be the partition
 of unity. Let $\tau_i > 0$ be a given number. For a subdomain $j \in \llbracket 1; N_i \rrbracket$, let*

$$G_{i,j} = D_{i,j} (R_{i,j} A_i R_{i,j}^\top) D_{i,j}.$$

Let $\tilde{P}_{i,j}$ be the projection on $\text{range}(R_{i,j} \tilde{A}_j R_{i,j}^\top)$ parallel to $\ker(R_{i,j} \tilde{A}_j R_{i,j}^\top)$. Let $K_{i,j} =$
 $\ker(R_{i,j} \tilde{A}_{i,j} R_{i,j}^\top)$, $L_{i,j} = \ker(G_{i,j}) \cap K_{i,j}$, and $L_{i,j}^{\perp K_{i,j}}$ the orthogonal complementary
 of $L_{i,j}$ in $K_{i,j}$. Consider the generalized eigenvalue problem:

$$(3.2) \quad \begin{aligned} \tilde{P}_{i,j} G_{i,j} \tilde{P}_{i,j} u_{i,j,k} &= \lambda_{i,j,k} R_{i,j} \tilde{A}_{i,j} R_{i,j}^\top u_{i,j,k}, \\ (u_{i,j,k}, \lambda_{i,j,k}) &\in \text{range}(R_{i,j} \tilde{A}_{i,j} R_{i,j}^\top) \times \mathbb{R}. \end{aligned}$$

Set

$$(3.3) \quad Z_{i,j} = L_{i,j}^{\perp K_{i,j}} \oplus \text{span}\{u_{i,j,k} \mid \lambda_{i,j,k} > \tau_i\}.$$

Then, the coarse space associated with LSPSPD matrices $\tilde{A}_{i,j}$ for $j = 1, \dots, N_i$ at level i
 is defined as:

$$(3.4) \quad \mathcal{S}_i = \bigoplus_{j=1}^{N_i} R_{i,j}^\top D_{i,j} Z_{i,j}.$$

Following notations from section 1, the columns of V_i span the coarse space \mathcal{S}_i . The
 matrix A_{i+1} is defined as:

$$(3.5) \quad A_{i+1} = V_i^\top A_i V_i.$$

The local SPSPD splitting matrices at level 1 will play an important role in the
 construction of the LSPSPD matrices at subsequent levels. In the following, we present
 an efficient approach for computing LSPSPD matrices for levels greater than 1.

4. Partitioning for levels strictly greater than 1. In this section, we explain
 how to obtain the partitioning sets $\Omega_{i,j,I}$ for $(i, j) \in \llbracket 2; L \rrbracket \times \llbracket 1; N_i \rrbracket$. Once the sets
 $\Omega_{i,j,\Gamma}$ for $j = 1, \dots, N_i$ are defined at level i , the following elements are readily
 available: sets $\Omega_{i,j,\Gamma}$, $\Omega_{i,j,\Delta}$, and $\Omega_{i,j}$; restriction operators $R_{i,j,I}$, $R_{i,j,\Gamma}$, $R_{i,j,\Delta}$, and
 $R_{i,j}$; permutation matrices $\mathcal{P}_{i,j}$ for $j = 1, \dots, N_i$.

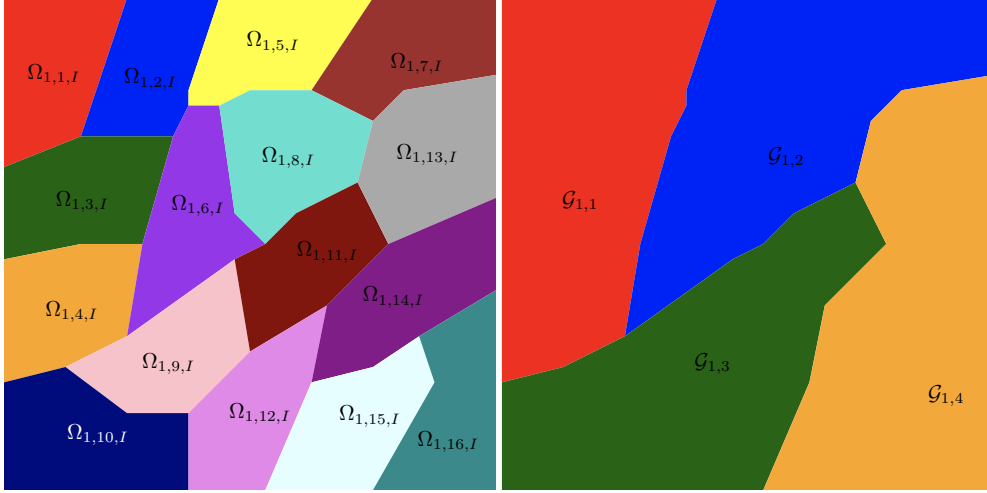


FIG. 4.1. Left: 16 subdomains at level 1. Right: 4 superdomains at level 1. $\mathcal{G}_{1,j} = \llbracket 4(j-1) + 1; 4(j-1) + 4 \rrbracket$.

338 **4.1. Superdomains as unions of several subdomains.** In this section, we
 339 introduce the notion of *superdomain*. It refers to the union of several neighboring
 340 subdomains. Let $\mathcal{G}_{i,1}, \dots, \mathcal{G}_{i,N_{i+1}}$ be disjoint subsets of $\llbracket 1; N_i \rrbracket$, where $\bigcup_{j=1}^{N_{i+1}} \mathcal{G}_{i,j} =$
 341 $\llbracket 1; N_i \rrbracket$. We call the union of the subdomains $\{k \in \llbracket 1; N_i \rrbracket : k \in \mathcal{G}_{i,j}\}$ superdomain j ,
 342 for $j = 1, \dots, N_{i+1}$. Figure 4.1 gives an example of how to set superdomains. Though
 343 this definition of superdomains may look somehow related to the fine mesh, it is in
 344 practice done at the algebraic level, as explained later on. Note that the indices of
 345 columns and rows of A_{i+1} are associated with the vectors contributed by the subdo-
 346 mains at level i in order to build the coarse space \mathcal{S}_i , see Figure 4.2. Hence, defining
 347 subdomains on the structure of A_{i+1} is natural once we have the subsets $\mathcal{G}_{i,j}$, for
 348 $j = 1, \dots, N_{i+1}$.

349 **4.2. Heritage from superdomains.** Let $e_{i,j}$ be the set of indices of the vectors
 350 that span $R_{i,j}^\top D_{i,j} Z_{i,j}$ in the matrix V_i for some $(i, j) \in \llbracket 1; L-1 \rrbracket \times \llbracket 1; N_i \rrbracket$, see
 351 Figure 4.2. We define $\Omega_{i+1,j,I} = \cup_{k \in \mathcal{G}_{i,j}} e_{i,k}$, for $j = 1, \dots, N_{i+1}$. We denote $\Omega_{i+1,j,\Gamma}$
 352 the subset of $\llbracket 1; n_{i+1} \rrbracket \setminus \Omega_{i+1,j,I}$ whose elements are at distance 1 from $\Omega_{i+1,j,I}$ through
 353 the graph of A_{i+1} . We note that

$$354 \quad \Omega_{i+1,j,\Gamma} \subset \bigcup_{p \in \mathcal{G}_{i,j}} \bigcup_{k \in \mathcal{V}_{i,p}} e_{i,k},$$

355 where $\mathcal{V}_{i,j}$ represents the set of subdomains that are neighbors of subdomain j at
 356 level i for $j = 1, \dots, N_i$. The overlapping subdomain j is defined by the set $\Omega_{i+1,j} =$
 357 $[\Omega_{i+1,j,I}, \Omega_{i+1,j,\Gamma}]$. The rest of the sets, restriction, and prolongation operators can
 358 be defined as given in section 1.

359 **5. LSPSD matrices for levels strictly greater than 1.** In [32, 12, 3], differ-
 360 ent methods are suggested to obtain local SPSP splitting matrices at level 1. These
 361 matrices are used to construct efficient two-level additive Schwarz preconditioners.
 362 Here in this section, we do not discuss the construction of these matrices at level 1. We
 363 suppose that we have the local SPSP matrices $\hat{A}_{1,j} \in \mathbb{R}^{n_1 \times n_1}$ for $j = 1, \dots, N_1$. We

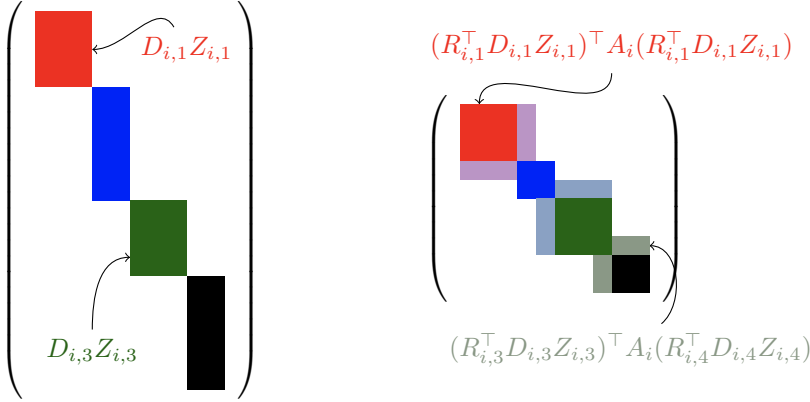


FIG. 4.2. Illustration of the correspondence of indices between the columns of V_i (left) and the rows and columns of A_{i+1} (right). Having no overlap in V_i is possible through a non-overlapping partition of unity.

364 focus on computing LSPSD matrices $\tilde{A}_{i,j} \in \mathbb{R}^{n_i \times n_i}$ for $(i,j) \in \llbracket 2; L \rrbracket \times \llbracket 1; N_i \rrbracket$. We also
 365 suppose that the coarse space \mathcal{S}_1 is available, i.e., the matrices V_1 and $A_2 = V_1^\top A_1 V_1$
 366 are known explicitly.

367 PROPOSITION 5.1. Let i be a fixed level index, and let $\tilde{A}_{i,j}$ be an LSPSD of A_i ,
 368 (see Definition 3.1), associated with subdomain j , for $j = 1, \dots, N_i$. Let $\mathcal{G}_{i,1}, \dots, \mathcal{G}_{i,N_{i+1}}$
 369 be a set of superdomains at level i associated with the partitioning at level $i+1$, see
 370 subsection 4.1. Let V_i^\top be the restriction matrix to the coarse space at level i . Then,
 371 the matrix $\tilde{A}_{i+1,j}$ which is defined as:

$$372 \quad \tilde{A}_{i+1,j} = \sum_{k \in \mathcal{G}_{i,j}} V_i^\top \tilde{A}_{i,k} V_i,$$

373 satisfies the conditions in Definition 3.1. That is, $\tilde{A}_{i+1,j}$ is LSPSD of A_{i+1} with
 374 respect to subdomain j for $j = 1, \dots, N_{i+1}$.

375 *Proof.* To prove that $\tilde{A}_{i+1,j}$ is LSPSD of A_{i+1} with respect to subdomain j , we
 376 have to prove the following:

- 377 • $R_{i+1,j,\Delta} \tilde{A}_{i+1,j} = 0$
- 378 • $u^\top \sum_{j=1}^{N_{i+1}} \tilde{A}_{i+1,j} u \leq k_{i+1} u^\top A_{i+1} u$ for all $u \in \mathbb{R}^{n_{i+1}}$.

379 First, note that $R_{i,k} \tilde{A}_{i,j} = 0$ for all non-neighboring subdomains k of subdomain j .
 380 This yields $Z_{i,k}^\top D_{i,k} R_{i,k} \tilde{A}_{i,j} = 0$ for these subdomains k .

381 Now, let $m \in \llbracket 1; n_{i+1} \rrbracket \setminus \Omega_{i+1,j}$. We will show that the m th row of $\tilde{A}_{i+1,j}$ is zero.
 382 Following the partitioning of subdomains at level $i+1$, there exists a subdomain Ω_{p_0}
 383 such that the m th column of V_i is part of $R_{i,p_0}^\top D_{i,p_0} Z_{i,p_0}$. We denote this column
 384 vector by v_m . Furthermore, the subdomain p_0 is not a neighbor of any subdomain
 385 that is a part of the superdomain $\mathcal{G}_{i,j}$. Hence, $v_m^\top \tilde{A}_{i,k} = 0$ for $k \in \mathcal{G}_{i,j}$. The m th row
 386 of $\tilde{A}_{i+1,j}$ is given as $v_m^\top \sum_{k \in \mathcal{G}_{i,j}} \tilde{A}_{i,k} V_i$. Then, $v_m^\top \sum_{k \in \mathcal{G}_{i,j}} \tilde{A}_{i,k} = 0$, and the m th row
 387 of $\tilde{A}_{i+1,j}$ is zero.

388 To prove the second condition, we have

$$389 \quad u^\top \sum_{j=1}^{N_{i+1}} \tilde{A}_{i+1,j} u = u^\top \sum_{j=1}^{N_{i+1}} \sum_{k \in \mathcal{G}_{i,j}} V_i^\top \tilde{A}_{i,k} V_i u.$$

390 Since $\{\mathcal{G}_{i,j}\}_{1 \leq j \leq N_{i+1}}$ form a disjoint partitioning of $\llbracket 1; N_i \rrbracket$, we can write

$$391 \quad u^\top \sum_{j=1}^{N_{i+1}} \tilde{A}_{i+1,j} u = u^\top \sum_{k=1}^{N_i} V_i^\top \tilde{A}_{i,k} V_i u,$$

$$392 \quad \leq u^\top V_i^\top \sum_{k=1}^{N_i} \tilde{A}_{i,k} V_i u.$$

393 $\tilde{A}_{i,k}$ is an LSPSD matrix of A_i for $k = 1, \dots, N_i$. Hence, we have

$$394 \quad u^\top \sum_{j=1}^{N_{i+1}} \tilde{A}_{i+1,j} u \leq k_i u^\top V_i^\top A_i V_i u,$$

$$395 \quad \leq k_i u^\top A_{i+1} u.$$

396 We finish the proof by setting $k_{i+1} = k_i$. \square

397 **Figure 5.1** gives an illustration of the LSPSD construction provided by **Proposition 5.1**. **Figure 5.1** (top left) represents the matrix A_1 . The graph of A_1 is partitioned into 16 subdomains. Each subdomain is represented by a different color. **Figure 5.1** (top right) represents the matrix V_1 whose column vectors form a basis of the coarse space \mathcal{S}_1 . Colors of columns of V_1 correspond to those of subdomains in A_1 . **Figure 5.1** (bottom left) represents the matrix $A_2 = V_1^\top A_1 V_1$. Note that column and row indices of A_2 are associated with column indices of V_1 . Four subdomains are used at level 2. The partitioning at level 2 is related to the superdomain $\mathcal{G}_{1,j} = \llbracket 4(j-1)+1; 4(j-1)+4 \rrbracket$ for $j = 1, \dots, 4$. **Figure 5.1** (bottom right) represents an LSPSD matrix of A_2 with respect to subdomain 1 at level 2.

398 **Theorem 5.2** shows that the third condition of the fictitious subspace lemma **Lemma 2.1** holds at level i for $i = 1, \dots, L$.

399 **THEOREM 5.2.** *Let $\tilde{A}_{i,j}$ be an LSPSD of A_i associated with subdomain j , for $(i, j) \in \llbracket 1; L \rrbracket \times \llbracket 1; N_i \rrbracket$. Let $\tau_i > 0$, $Z_{i,j}$ be the subspace associated with $\tilde{A}_{i,j}$, and $P_{i,j}$ be the projection on $Z_{i,j}$ as defined in **Lemma 2.5**. Let $u_i \in \mathbb{R}^{n_i}$ and let $u_{i,j} = (D_{i,j} (I_{n_{i,j}} - P_{i,j}) R_{i,j} u_i)$ for $(i, j) \in \llbracket 1; L \rrbracket \times \llbracket 1; N_i \rrbracket$. Let $u_{i,0}$ be defined as,*

$$400 \quad u_{i,0} = (V_i^\top V_i)^{-1} V_i^\top \left(\sum_{j=1}^{N_i} R_{i,j}^\top D_{i,j} P_{i,j} R_{i,j} u_i \right).$$

401 Let $m_i = (2 + (2k_{i,c} + 1)k_i \tau_i)^{-1}$. Then,

$$402 \quad u_i = \sum_{j=0}^{N_i} R_{i,j}^\top u_{i,j},$$

403 and

$$404 \quad (5.1) \quad m_i \sum_{j=0}^{N_i} u_{i,j}^\top R_{i,j} A_i R_{i,j}^\top u_{i,j} \leq u_i^\top A_i u_i.$$

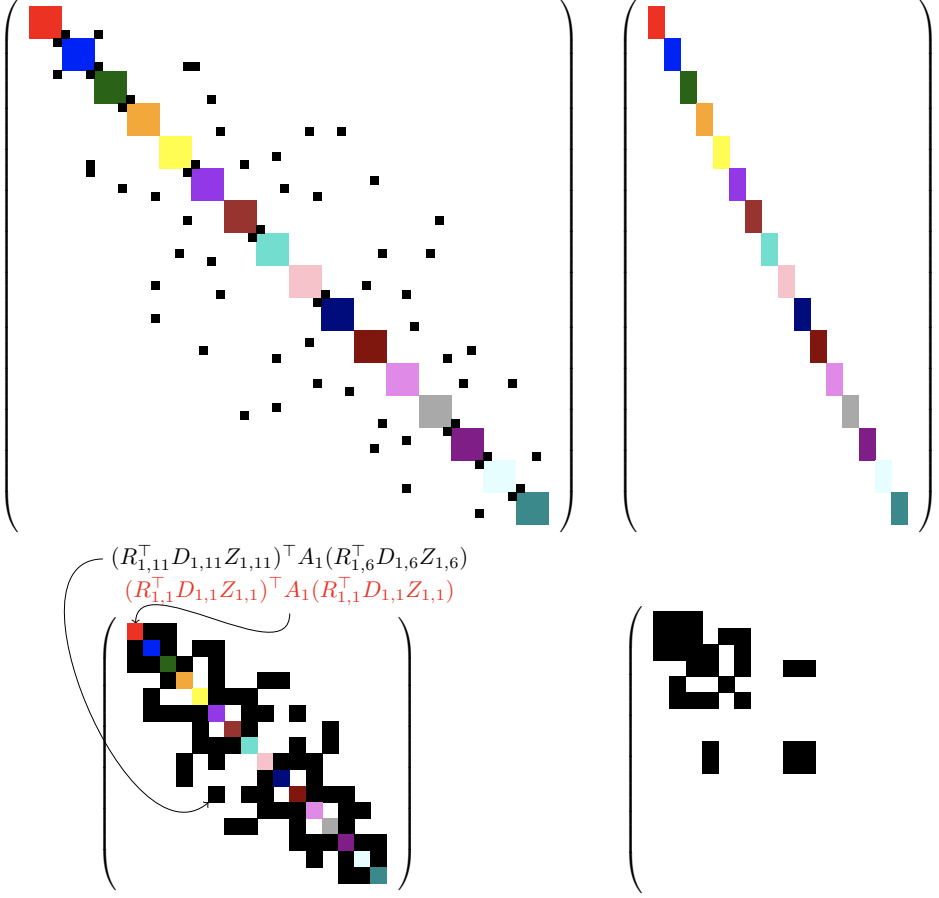


FIG. 5.1. Illustration of the LSPSD construction provided by Proposition 5.1. Top left: the matrix A_1 , top right: V_1 , bottom left: the matrix $A_2 = V_1^\top A_1 V_1$, bottom right: $\tilde{A}_{2,1} = \sum_{j \in \mathcal{G}_{1,1}} V_1^\top \tilde{A}_{1,j} V_1$, where $\mathcal{G}_{1,1} = 1, \dots, 4$

421 *Proof.* We have

$$422 \quad \sum_{j=0}^{N_i} R_{i,j}^\top u_{i,j} = V_i (V_i^\top V_i)^{-1} V_i^\top \left(\sum_{j=1}^{N_i} R_{i,j}^\top D_{i,j} P_{i,j} R_{i,j} u_i \right) + \sum_{j=1}^{N_i} R_{i,j}^\top u_{i,j}$$

423

424 Since for all $y \in \mathcal{S}_i$, $V_i (V_i^\top V_i)^{-1} V_i^\top y = y$, we have

$$425 \quad \sum_{j=0}^{N_i} R_{i,j}^\top u_{i,j} = \sum_{j=1}^{N_i} R_{i,j}^\top D_{i,j} P_{i,j} R_{i,j} u_i + \sum_{j=1}^{N_i} R_{i,j}^\top (D_{i,j} (I_{n_{i,j}} - P_{i,j}) R_{i,j} u_i),$$

$$426 \quad = \sum_{j=1}^{N_i} R_{i,j}^\top D_{i,j} R_{i,j} u_i,$$

$$427 \quad = u_i.$$

429 To prove the inequality (5.1), we start with the inequality from Lemma 2.4. We

430 have

$$431 \quad (5.2) \quad \sum_{j=0}^{N_i} u_{i,j}^\top R_{i,j} A_i R_{i,j}^\top u_{i,j} \leq 2u_i^\top A_i u_i + (2k_{i,c} + 1) \sum_{j=1}^{N_i} u_{i,j}^\top R_{i,j} A_i R_{i,j}^\top u_{i,j},$$

433 where we chose $u_{\mathcal{B}_i}$ in [Lemma 2.4](#) to be $(u_{i,j})_{j=0,\dots,N_i}$ and $u_{A_i} = u_i$. In [Definition 3.2](#),
434 we defined $Z_{i,j}$, such that for all $w \in \mathbb{R}^{n_{i,j}}$ we have

$$435 \quad ((I_{n_{i,j}} - P_{i,j})w)^\top (D_{i,j} R_{i,j} A_i R_{i,j}^\top D_{i,j}) ((I_{n_{i,j}} - P_{i,j})w) \leq \tau_i w^\top (R_{i,j} \tilde{A}_{i,j} R_{i,j}^\top) w.$$

437 Hence, in the special case $w = R_{i,j} u_i$, we can write

$$438 \quad ((I_{n_{i,j}} - P_{i,j})R_{i,j} u_i)^\top (D_{i,j} R_{i,j} A_i R_{i,j}^\top D_{i,j}) ((I_{n_{i,j}} - P_{i,j})R_{i,j} u_i) \\ 439 \quad \leq \tau_i (R_{i,j} u_i)^\top (R_{i,j} \tilde{A}_{i,j} R_{i,j}^\top) (R_{i,j} u_i).$$

442 Equivalently,

$$443 \quad u_{i,j}^\top R_{i,j} A_i R_{i,j}^\top u_{i,j} \leq \tau_i (R_{i,j} u_i)^\top R_{i,j} \tilde{A}_{i,j} R_{i,j}^\top (R_{i,j} u_i).$$

445 Plugging this inequality in (5.2) gives

$$446 \quad \sum_{j=0}^{N_i} u_{i,j}^\top R_{i,j} A_i R_{i,j}^\top u_{i,j} \leq 2u_i^\top A_i u_i + (2k_{i,c} + 1) \tau_i \sum_{j=1}^{N_i} (R_{i,j} u_i)^\top R_{i,j} \tilde{A}_{i,j} R_{i,j}^\top (R_{i,j} u_i).$$

448 Since $\tilde{A}_{i,j}$ is local, we have

$$449 \quad (R_{i,j} u_i)^\top R_{i,j} \tilde{A}_{i,j} R_{i,j}^\top (R_{i,j} u_i) = u_i^\top \tilde{A}_{i,j} u_i, \text{ for } j = 1, \dots, N_i.$$

450 By using the fact that $\tilde{A}_{i,j}$ is LSPSD of A_i for $j = 1, \dots, N_i$, we obtain the following:

$$451 \quad \sum_{j=0}^{N_i} u_{i,j}^\top R_{i,j} A_i R_{i,j}^\top u_{i,j} \leq 2u_i^\top A_i u_i + (2k_{i,c} + 1) k_i \tau_i u_i^\top A_i u_i.$$

453 Multiplying both sides with m_i ends the proof, i.e.,

$$454 \quad m_i \sum_{j=0}^{N_i} u_{i,j}^\top R_{i,j} A_i R_{i,j}^\top u_{i,j} \leq u_i^\top A_i u_i. \quad \square$$

456 [Theorem 5.3](#) provides an upper bound on the condition number of the preconditioned matrix $M_i^{-1} A_i$ for $i = 1, \dots, L$.

458 **THEOREM 5.3.** *Let M_i be the additive Schwarz preconditioner at level i combined*
459 *with the coarse space correction induced by \mathcal{S}_i defined in (3.4). The following inequality*
460 *holds,*

$$461 \quad \kappa(M_i^{-1} A_i) \leq (k_{i,c} + 1) (2 + (2k_{i,c} + 1) k_i \tau_i).$$

462 *Proof.* [Lemma 2.2](#), [Lemma 2.3](#), and [Theorem 5.2](#) prove that the multilevel preconditioner verifies the conditions in [Lemma 2.1](#) at each level i . Hence, the spectrum of the preconditioned matrix $M_i^{-1} A_i$ is contained in the interval $[(2 + (2k_{i,c} + 1) k_i \tau_i)^{-1}, k_{i,c} + 1]$. Equivalently, the condition number of the preconditioned matrix at level i verifies the following inequality

$$467 \quad \kappa(M_i^{-1} A_i) \leq (k_{i,c} + 1) (2 + (2k_{i,c} + 1) k_i \tau_i). \quad \square$$

468 **Proposition 5.1** shows that the constant k_i associated with the LSPSD matrices at
 469 level i is independent of the number of levels and bounded by the number of subdo-
 470 mains at level 1. Indeed,

$$471 \quad k_1 \geq k_i \text{ for } i = 2, \dots, L.$$

472 Furthermore, in the case where the LSPSD matrices at the first level are the Neumann
 473 matrices, k_i is bounded by the maximum number of subdomains at level 1 that share
 474 an unknown.

475 The constant $k_{i,c}$ for $i = 1, \dots, L$ is the minimum number of distinct colors so that
 476 $\{\text{span}\{R_{i,j}^\top\}\}_{1 \leq j \leq N_i}$ of the same color are mutually A_i -orthogonal. Both constants
 477 k_i and $k_{i,c}$ are independent of the number of subdomains for each level i .

478 The constant τ_i can be chosen such that the condition number of the preconditioned
 479 system at level i is upper bounded by a prescribed value. Hence, this allows
 480 to have a robust convergence of the preconditioned Krylov solver at each level.

481 Algorithm 5.1 presents the construction of the multilevel additive Schwarz method
 482 by using GenEO. The algorithm iterates over the levels. At each level, three main
 483 operations are performed. First, the construction of the LSPSD matrices. At level 1,
 484 the LSPSD matrices are the Neumann matrices, otherwise, **Proposition 5.1** is used
 485 to compute them. Once the LSPSD matrix is available, the generalized eigenvalue
 486 problem in (3.2) has to be solved concurrently. Given the prescribed upper bound on
 487 the condition number, $Z_{i,j}$ can be set. Finally, the coarse space is available and the
 coarse matrix is assembled.

Algorithm 5.1 Multilevel GenEO

Require: $A_1 = A \in \mathbb{R}^{n \times n}$ SPD, $L + 1$ number of levels, N_i number of subdomains
 at each level, $\mathcal{G}_{i,j}$ sets of superdomains

Ensure: preconditioner at each level i , M_i^{-1} with bounded condition number of
 $M_i^{-1}A_i$

- 1: **for** $i = 1, \dots, L$ **do**
- 2: **for** each subdomain $j = 1, \dots, N_i$ **do**
- 3: $A_{i,j} = R_{i,j}A_iR_{i,j}^\top$ (*local matrix associated with subdomain j*)
- 4: **if** $i = 1$ **then**
- 5: local SPSD $\tilde{A}_{i,j}$ is Neumann matrix of subdomain j
- 6: **else**
- 7: compute local SPSD matrix as

$$\tilde{A}_{i,j} = \sum_{k \in \mathcal{G}_{i,j}} V_{i-1}^\top \tilde{A}_{i-1,k} V_{i-1}$$

- 8: **end if**
 - 9: solve the generalized eigenvalue problem (3.2), set $Z_{i,j}$ as in (3.3)
 - 10: **end for**
 - 11: $\mathcal{S}_i = \bigoplus_{j=1}^{N_i} D_{i,j}R_{i,j}^\top Z_{i,j}$, V_i basis of \mathcal{S}_i
 - 12: coarse matrix $A_{i+1} = V_i^\top A_i V_i$, $A_{i+1} \in \mathbb{R}^{n_{i+1} \times n_{i+1}}$
 - 13: **end for**
 - 14: $M_i^{-1} = V_i A_{i+1}^{-1} V_i^\top + \sum_{j=1}^{N_i} R_{i,j}^\top A_{i,j}^{-1} R_{i,j}$
-

488

489 **6. Numerical experiments.** In this section, the developed theory is validated
 490 numerically with FreeFEM [14] for finite element discretizations and HPDDM [19]

491 for domain decomposition methods. We present numerical experiments on two highly
 492 challenging problems illustrating the efficiency and practical usage of the proposed
 493 method. For both problems, we use $N_1 = 2,048$ MPI processes (equal to the number
 494 of subdomains at level 1). We compare the two-level GenEO preconditioner and its
 495 multilevel extension by varying N_2 between 4 and 256. For the two-level method,
 496 N_2 corresponds to the number of MPI processes that solve the coarse problem in a
 497 distributed fashion using MKL CPARDISO [17]. For the multilevel method, N_3 is
 498 set to 1, i.e., a three-level method is used. The goal of these numerical experiments
 499 is to show that when one switches from a two-level method with an exact coarse
 500 solver, to our proposed multilevel method, the number of outer iterations is not im-
 501 pacted. Thus, three levels are sufficient. As an outer solver, since all levels but the
 502 coarsest are solved approximately, the flexible GMRES [30] is used. It is stopped
 503 when relative unpreconditioned residuals are lower than 10^{-6} . Subdomain matrices
 504 $\{A_{i,j}\}_{1 \leq i \leq 2, 1 \leq j \leq N_i}$ are factorized concurrently using MKL PARDISO, and eigenvalue
 505 problems are solved using ARPACK [24]. In both, two- and three-level GenEO, we
 506 factorize the local matrices $A_{1,j}$ for $j \in \llbracket 1; N_1 \rrbracket$ and solve the generalized eigenvalue
 507 problems concurrently at the first level. For this reason, we do not take into account
 508 the time needed for these two steps which are performed without any communication
 509 between MPI processes. We compare the time needed to assemble and factorize A_2
 510 in the two-level approach against the time needed to assemble A_2 and local SPSD
 511 matrices $\tilde{A}_{2,j}$ for $j \in \llbracket 1; N_2 \rrbracket$, solve the generalized eigenvalue problems concurrently
 512 on the second level, assemble, and factorize the matrix A_3 in the three-level approach.
 513 We also compare the time spent in the outer Krylov solver during the solution phase.
 514 Readers interested by a comparison of the efficiency of GenEO and multigrid methods
 515 such as GAMG [1] are referred to [18]. FreeFEM scripts used to produce the following
 516 results are available at the following URL: <https://github.com/prj-/aldaas2019multi>¹.

517 **6.1. Diffusion test cases.** The scalar diffusion equation with highly heteroge-
 518 neous coefficient κ is solved in $[0, 1]^d$ ($d = 2$ or 3). The strong formulation of the
 519 equation is:

$$\begin{aligned} -\nabla \cdot (\kappa \nabla u) &= 1 && \text{in } \Omega, \\ u &= 0 && \text{on } \Gamma_D, \\ \frac{\partial u}{\partial n} &= 0 && \text{on } \Gamma_N. \end{aligned}$$

522 The exterior normal vector to the boundary of Ω is denoted n . Γ_D is the subset
 523 of the boundary of Ω corresponding to $x = 0$ in 2D and 3D. Γ_N is defined as the
 524 complementary of Γ_D with respect to the boundary of Ω . We discretize the equation
 525 using \mathbb{P}_2 and \mathbb{P}_4 finite elements in the 3D and 2D test cases, respectively. The number
 526 of unknowns is 441×10^6 and 784×10^6 , with approximately 28 and 24 nonzero elements
 527 per row in the 3D and 2D cases, respectively. The heterogeneity is due to the jumps
 528 in the diffusion coefficient κ , see Figure 6.1, which is modeled with the following \mathbb{P}_0
 529 function:

$$\kappa = \begin{cases} 10^5([9y]) & \text{if } [9x] \equiv [9y] \equiv 0 \pmod{2}, \\ 1 & \text{elsewhere.} \end{cases}$$

531 The results in two dimensions are reported in Table 6.1. The number of outer itera-
 532 tions for both two- and three-level GenEO is 32. The size of the level 2 operator is

¹note to reviewers: the repository is not yet public but will be once the paper is accepted

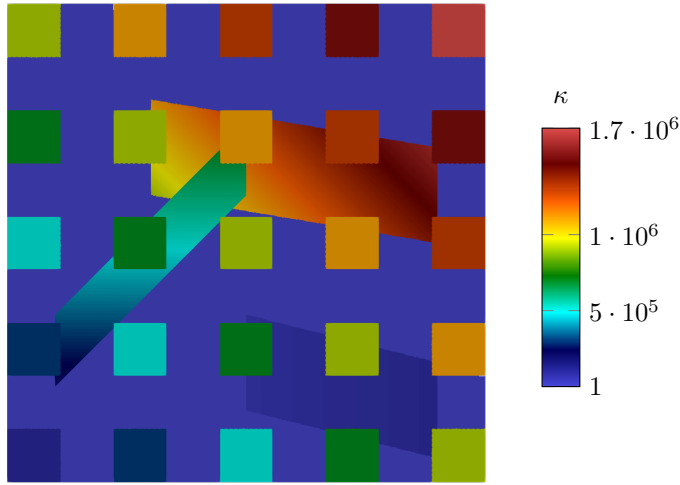


FIG. 6.1. Variation of the coefficient κ used for the diffusion test case

N_2	two-level GenEO		three-level GenEO		
	CS	solve	CS	solve	inner iter
4	2.4	11.9	6.5	27.4	14
16	1.8	11.3	3.6	15.4	15
64	1.9	12.1	3.0	16.7	14
256	2.4	18.4	2.8	13.9	13

TABLE 6.1

Diffusion 2D test case, comparison between two- and three-level GenEO

533 $n_2 = 25 \times 2,048 = 51,200$. It is striking that the multilevel method does not deteri-
 534 orate the numerical performance of the outer solver. For the two-level method, the
 535 first column corresponds to the time needed to assemble the Galerkin operator A_2
 536 from (3.5) (assuming V_1 has already been computed by ARPACK), and to factorize it
 537 using N_2 MPI processes. For the three-level method, the first column corresponds to
 538 the time needed to assemble level 2 local subdomain matrices $\{A_{2,j}\}_{1 \leq j \leq N_2}$, level 2
 539 local SPSD matrices, solve the generalized eigenvalue problem (3.2) concurrently, as-
 540 semble the Galerkin operator A_3 and factorize it on a single process. The size of
 541 the level 3 operator is $n_3 = 20 \times N_2$. For both two- and three-level methods, the
 542 second column is the time spent in the outer Krylov solver once the preconditioner
 543 has been set up. In the last column of the three-level method, the number of inner
 544 iterations for solving systems involving A_2 , which is not inverted exactly anymore,
 545 is reported. Another important numerical property of our method is that, thanks to
 546 fully controlled bounds at each level, the number of inner iterations is low, indepen-
 547 dently of the number of superdomains N_2 . Because this problem is not large enough,
 548 it is still tractable by a two-level method, for which HPDDM was highly optimized
 549 for. Thus, there is no performance gain to be expected at this scale. However, one
 550 can notice that the construction of the coarse operator(s) scales nicely with N_2 for
 551 the three-level method, whereas the performance of the direct solver MKL CPARDISO
 552 quickly plateaus because of the finer and finer parallel workload granularity.

553 The results in three dimensions are reported in Table 6.2. The number of outer

N_2	two-level GenEO		three-level GenEO		
	CS	solve	CS	solve	inner iter
4	7.0	20.9	16.9	43.6	17
16	5.0	19.8	7.7	26.7	17
64	5.1	20.1	5.8	32.7	15
256	5.2	24.1	5.3	22.6	14

TABLE 6.2

Diffusion 3D test case, comparison between two- and three-level GenEO

554 iterations for both the two- and three-level GenEO is 19. The observations made
 555 in two dimensions still hold, and the dimensions of A_2 and A_3 are the same. Once
 556 again, it is important to note that the number of outer iterations is the same for both
 557 methods.

558 **6.2. Linear elasticity test cases.** The system of linear elasticity with highly
 559 heterogeneous elastic moduli is solved in 2D and 3D. The strong formulation of the
 560 equation is given as:

$$\begin{aligned}
 (6.1) \quad & \operatorname{div} \sigma(u) + f = 0 \quad \text{in } \Omega, \\
 & u = 0 \quad \text{on } \Gamma_D, \\
 & \sigma(u) \cdot n = 0 \quad \text{on } \Gamma_N.
 \end{aligned}$$

563 The physical domain Ω is a beam of dimensions $[0, 10] \times [0, 1]$, extruded for $z \in$
 564 $[0, 1]$ in 3D. The Cauchy stress tensor $\sigma(\cdot)$ is given by Hooke's law: it can be expressed
 565 in terms of Young's modulus E and Poisson's ratio ν .

$$\sigma_{ij}(u) = \begin{cases} 2\mu\varepsilon_{ij}(u) & i \neq j, \\ 2\mu\varepsilon_{ii}(u) + \lambda\operatorname{div}(u) & i = j, \end{cases}$$

567 where

$$\varepsilon_{ij}(u) = \frac{1}{2} \left(\frac{\partial u_i}{\partial x_j} + \frac{\partial u_j}{\partial x_i} \right), \mu = \frac{E}{2(1+\nu)}, \text{ and } \lambda = \frac{E\nu}{1-2\nu}.$$

569 The exterior normal vector to the boundary of Ω is denoted n . Γ_D is the subset
 570 of the boundary of Ω corresponding to $x = 0$ in 2D and 3D. Γ_N is defined as the
 571 complementary of Γ_D with respect to the boundary of Ω . We discretize (6.1) using
 572 the following vectorial finite elements: $(\mathbb{P}_2, \mathbb{P}_2, \mathbb{P}_2)$ in 3D and $(\mathbb{P}_3, \mathbb{P}_3)$ in 2D. The
 573 number of unknowns is 146×10^6 and 847×10^6 , with approximately 82 and 34
 574 nonzero elements per row in the 3D and 2D cases, respectively. The heterogeneity is
 575 due to the jumps in E and ν . We consider discontinuous piecewise constant values
 576 for E and ν : $(E_1, \nu_1) = (2 \times 10^{11}, 0.25)$, $(E_2, \nu_2) = (10^7, 0.45)$, see Figure 6.2.

577 Results in two (resp. three) dimensions are reported in Table 6.3 (resp. Table 6.4).
 578 The number of outer iterations are 73 and 45 respectively. For these test cases, we
 579 slightly relaxed the criterion for selecting eigenvectors in coarse spaces, which explains
 580 why the iteration counts increase. However, the same observations as for the diffusion
 581 test cases still hold. The dimension of the level 2 matrix is $n_2 = 50 \times 2,048 = 1.02 \cdot 10^5$,
 582 while for the level 3 matrix it is $n_3 = 20 \times N_2$. We observe that the number of iterations
 583 of the inner solver increases slowly when increasing the number of subdomains from
 584 4 to 256 in the 2D case and remains almost constant in the 3D case. In terms of

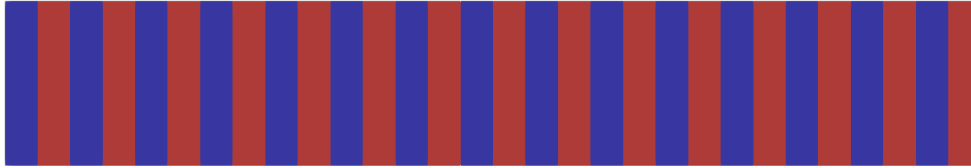


FIG. 6.2. Variation of the structure coefficients used for the elasticity test case

N_2	two-level GenEO		three-level GenEO		
	CS	solve	CS	solve	inner iter
4	4.8	52.7	22.5	179.3	31
16	3.9	50.3	9.3	124.9	57
64	4.0	53.1	7.2	71.5	34
256	4.8	63.2	6.8	71.2	44

TABLE 6.3

Elasticity 2D test case, comparison between two- and three-level GenEO

585 runtime, the two-level GenEO is faster than three-level GenEO for these matrices of
 586 medium dimensions.

587 To show the potential of our method at larger scales, a three-dimensional linear
 588 elasticity problem of size 616×10^6 is now solved on $N_1 = 8,192$ processes and $N_2 = 256$
 589 superdomains. With the two-level method, A_2 is assembled and factorized in 27.5
 590 seconds. With the three-level method, this step now takes 13.2 seconds, see Table 6.5.
 591 Once again, as before, the number of outer iterations remains constant and equal to
 592 53 for both methods. Not taking into account the preconditioner setup, the problem is
 593 solved in 52 seconds in both cases. At this regime, it is clear that there are important
 594 gains for the setup phase. At even greater scales, gains for the solution phase are
 595 also expected. Moreover, another interesting fact to note regarding computation time
 596 is that the generalized eigenvalue problems solved concurrently at the first level to
 597 obtain V_1 actually represents a significant part of the total time of 152.8 seconds (resp.
 598 138.5 seconds) with the two- (resp. three-)level method: 113.3 seconds. This cost can
 599 be reduced by taking a larger number of (smaller) subdomains, with the drawback of
 600 increasing the size of V_1 and thus A_2 . This drawback represents a clear bottleneck
 601 for the two-level method but is alleviated by using the three-level method, making it
 602 a good candidate for problems at greater scales.

603 **7. Conclusion.** In this paper, we reviewed generalities of overlapping Schwarz
 604 preconditioners and presented a framework for its multilevel extension. We generalized
 605 the local SPSD splitting presented in [3] to cover a larger set of matrices leading to
 606 more flexibility for building robust coarse spaces. Based on local SPSD matrices
 607 on the first level, we presented how to compute local SPSD matrices for coarser
 608 levels. The multilevel solver based on hierarchical local SPSD matrices is robust and
 609 guarantees a bound on the condition number of the preconditioned matrix at each
 610 level depending on predefined values. Numerical experiments illustrate the theory and
 611 prove the efficiency of the method on challenging problems of large size arising from
 612 heterogeneous linear elasticity and diffusion problems with jumps in the coefficients
 613 of multiple orders of magnitude.

N_2	two-level GenEO		three-level GenEO		
	CS	solve	CS	solve	inner iter
4	28.5	46.9	78.9	296.7	23
16	17.3	35.4	24.5	124.5	23
64	15.0	33.2	15.4	62.2	21
256	13.6	40.7	10.6	50.7	23

TABLE 6.4

Elasticity 3D test case, comparison between two- and three-level GenEO

N_2	two-level GenEO		three-level GenEO		
	CS	solve	CS	solve	inner iter
256	27.5	52.0	13.2	52.0	25

TABLE 6.5

Elasticity 3D test case, comparison between two- and three-level GenEO

614 **8. Acknowledgements.** This work was granted access to the HPC resources of
615 TGCC@CEA under the allocation A0050607519 made by GENCI. The work of the
616 second author was supported by the NLAFFET project as part of European Union’s
617 Horizon 2020 research and innovation program under grant 671633.

618

REFERENCES

- 619 [1] M. F. ADAMS, H. H. BAYRAKTAR, T. M. KEAVENY, AND P. PAPADOPOULOS, *Ultrascaleable*
620 *Implicit Finite Element Analyses in Solid Mechanics with over a Half a Billion Degrees of*
621 *Freedom*, in Proceedings of the 2004 ACM/IEEE Conference on Supercomputing, SC ’04,
622 IEEE Computer Society, 2004.
- 623 [2] M. F. ADAMS AND J. W. DEMMEL, *Parallel Multigrid Solver for 3D Unstructured Finite El-*
624 *ement Problems*, in Proceedings of the 1999 ACM/IEEE Conference on Supercomputing,
625 SC ’99, ACM, 1999.
- 626 [3] H. AL DAAS AND L. GRIGORI, *A class of efficient locally constructed preconditioners based on*
627 *coarse spaces*, SIAM Journal on Matrix Analysis and Applications, 40 (2019), pp. 66–91.
- 628 [4] S. BADIA, A. MARTÍN, AND J. PRINCIPE, *Multilevel balancing domain decomposition at extreme*
629 *scales*, SIAM Journal on Scientific Computing, 38 (2016), pp. C22–C52.
- 630 [5] P. E. BJØRSTAD, M. J. GANDER, A. LONELAND, AND T. RAHMAN, *Does SHER for Additive*
631 *Schwarz Work Better than Predicted by Its Condition Number Estimate?*, in International
632 Conference on Domain Decomposition Methods, Springer, 2017, pp. 129–137.
- 633 [6] A. BORZÌ, V. DE SIMONE, AND D. DI SERAFINO, *Parallel algebraic multilevel Schwarz precon-*
634 *ditioners for a class of elliptic PDE systems*, Computing and Visualization in Science, 16
635 (2013), pp. 1–14.
- 636 [7] M. BREZINA, A. CLEARY, R. FALGOUT, V. HENSON, J. JONES, T. MANTEUFFEL, S. MCCORMICK,
637 AND J. RUGE, *Algebraic Multigrid Based on Element Interpolation (AMGe)*, SIAM Journal
638 on Scientific Computing, 22 (2001), pp. 1570–1592.
- 639 [8] X.-C. CAI AND M. SARKIS, *A restricted additive Schwarz preconditioner for general sparse*
640 *linear systems*, SIAM Journal on Scientific Computing, 21 (1999), pp. 792–797.
- 641 [9] T. F. CHAN AND T. P. MATHEW, *Domain decomposition algorithms*, Acta Numerica, 3 (1994),
642 pp. 61–143.
- 643 [10] T. CHARTIER, R. D. FALGOUT, V. E. HENSON, J. JONES, T. MANTEUFFEL, S. MCCORMICK,
644 J. RUGE, AND P. S. VASSILEVSKI, *Spectral AMGe (ρ AMGe)*, SIAM Journal on Scientific
645 Computing, 25 (2003), pp. 1–26.
- 646 [11] C. CHEVALIER AND F. PELLEGRINI, *PT-SCOTCH: A tool for efficient parallel graph ordering*,
647 Parallel Computing, 34 (2008), pp. 318–331. Parallel Matrix Algorithms and Applications.
- 648 [12] V. DOLEAN, P. JOLIVET, AND F. NATAF, *An introduction to domain decomposition methods*,
649 Society for Industrial and Applied Mathematics, 2015. Algorithms, theory, and parallel
650 implementation.

- 651 [13] M. GRIEBEL AND P. OSWALD, *On the abstract theory of additive and multiplicative Schwarz*
652 *algorithms*, Numerische Mathematik, 70 (1995), pp. 163–180.
- 653 [14] F. HECHT, *New development in FreeFem++*, Journal of Numerical Mathematics, 20 (2012),
654 pp. 251–266.
- 655 [15] A. HEINLEIN, A. KLOWONN, O. RHEINBACH, AND F. RÖVER, *A Three-Level Extension of the*
656 *GDSW Overlapping Schwarz Preconditioner in Three Dimensions*, technical report, Uni-
657 versität zu Köln, November 2018.
- 658 [16] V. E. HENSON AND U. M. YANG, *BoomerAMG: A parallel algebraic multigrid solver and pre-*
659 *conditioner*, Applied Numerical Mathematics, 41 (2002), pp. 155–177. Developments and
660 Trends in Iterative Methods for Large Systems of Equations.
- 661 [17] INTEL, *MKL web page*. <https://software.intel.com/en-us/intel-mkl>, 2019.
- 662 [18] P. JOLIVET, *Domain decomposition methods. Application to high-performance computing*, the-
663 ses, Université de Grenoble, Oct. 2014.
- 664 [19] P. JOLIVET, F. HECHT, F. NATAF, AND C. PRUD'HOMME, *Scalable domain decomposition pre-*
665 *conditioners for heterogeneous elliptic problems*, in Proceedings of the International Con-
666 ference on High Performance Computing, Networking, Storage and Analysis, SC13, ACM,
667 2013.
- 668 [20] J. JONES AND P. VASSILEVSKI, *AMGe Based on Element Agglomeration*, SIAM Journal on
669 Scientific Computing, 23 (2001), pp. 109–133.
- 670 [21] D. KALCHEV, C. LEE, U. VILLA, Y. EFENDIEV, AND P. VASSILEVSKI, *Upscaling of mixed finite*
671 *element discretization problems by the spectral AMGe method*, SIAM Journal on Scientific
672 Computing, 38 (2016), pp. A2912–A2933.
- 673 [22] G. KARYPIS AND V. KUMAR, *Multilevel k-way partitioning scheme for irregular graphs*, Journal
674 of Parallel and Distributed Computing, 48 (1998), pp. 96–129.
- 675 [23] F. KONG AND X.-C. CAI, *A highly scalable multilevel Schwarz method with boundary geometry*
676 *preserving coarse spaces for 3D elasticity problems on domains with complex geometry*,
677 SIAM Journal on Scientific Computing, 38 (2016), pp. C73–C95.
- 678 [24] R. LEHOUCQ, D. SORENSEN, AND C. YANG, *ARPACK users' guide: solution of large-scale*
679 *eigenvalue problems with implicitly restarted Arnoldi methods*, vol. 6, Society for Industrial
680 and Applied Mathematics, 1998.
- 681 [25] J. MANDEL, B. SOUSEDIK, AND C. R. DOHRMANN, *Multispace and multilevel BDDC*, Comput-
682 ing, 83 (2008), pp. 55–85.
- 683 [26] O. MARQUES, A. DRUINSKY, X. S. LI, A. T. BARKER, P. VASSILEVSKI, AND D. KALCHEV, *Tuning*
684 *the coarse space construction in a spectral AMG solver*, Procedia Computer Science, 80
685 (2016), pp. 212–221. International Conference on Computational Science 2016, ICCS 2016,
686 6–8 June 2016, San Diego, California, USA.
- 687 [27] S. V. NEPOMNYASCHIKH, *Mesh theorems of traces, normalizations of function traces and their*
688 *inversions*, Russian Journal of Numerical Analysis and Mathematical Modelling, 6 (1991),
689 pp. 1–25.
- 690 [28] ———, *Decomposition and fictitious domains methods for elliptic boundary value problems*,
691 1992.
- 692 [29] Y. NOTAY, *An aggregation-based algebraic multigrid method*, Electronic Transactions on Nu-
693 merical Analysis, 37 (2010), pp. 123–146.
- 694 [30] Y. SAAD., *A Flexible Inner–Outer Preconditioned GMRES Algorithm*, SIAM Journal on Sci-
695 entific Computing, 14 (1993), pp. 461–469.
- 696 [31] Y. SAAD, *Iterative Methods for Sparse Linear Systems*, Society for Industrial and Applied
697 Mathematics, 2nd ed., 2003.
- 698 [32] N. SPILLANE, V. DOLEAN, P. HAURET, F. NATAF, C. PECHSTEIN, AND R. SCHEICHL, *Abstract*
699 *robust coarse spaces for systems of PDEs via generalized eigenproblems in the overlaps*,
700 Numerische Mathematik, 126 (2014), pp. 741–770.
- 701 [33] A. TOSELLI AND O. WIDLUND, *Domain Decomposition Methods - Algorithms and Theory*,
702 Springer Series in Computational Mathematics, Springer Berlin Heidelberg, 2005.
- 703 [34] J. XU, *Theory of Multilevel Methods*, PhD thesis, Cornell University, 1989.
- 704 [35] S. ZAMPINI, *PCBDDC: A class of robust dual-primal methods in PETSc*, SIAM Journal on
705 Scientific Computing, 38 (2016), pp. S282–S306.